# Copper-Dependent Cytotoxicity of 8-Hydroxyquinoline Derivatives Correlates with Their Hydrophobicity and Does Not Require Caspase Activation

Saverio Tardito,[‡,§,∥] Amelia Barilli,[‡,§] Irene Bassanetti,[†] Matteo Tegoni,[†] Ovidio Bussolati,[‡] Renata Franchi-Gazzola,[‡] Claudio Mucchino,[†] and Luciano Marchiò*[,†]

[†]Dipartimento di Chimica, Università degli Studi di Parma, Viale delle Scienze 17/A, 43123 Parma, Italy

[‡]Dipartimento di Scienze Biomediche, Biotecnologiche e Traslazionali, Università degli Studi di Parma, Via Volturno 39, 43100 Parma, Italy

S Supporting Information

ABSTRACT: This study reports the structure−activity relationship of a series of 8-hydroxoquinoline derivatives (8-HQs) and focuses on the cytotoxic activity of 5-Cl-7-I-8-HQ (clioquinol, CQ) copper complex (Cu(CQ)). 8-HQs alone cause a dose-dependent loss of viability of the human tumor HeLa and PC3 cells, but the coadminstration of copper increases the ligands effects, with extensive cell death occurring in both cell lines. Cytotoxic doses of Cu(CQ) promote intracellular copper accumulation and massive endoplasmic reticulum vacuolization that precede a nonapoptotic (para-ptotic) cell death. The cytotoxic effect of Cu(CQ) is reproduced in normal human endothelial cells (HUVEC) at concentrations double those effective in tumor cells, pointing

to a potential therapeutic window for Cu(CQ). Finally, the results show that the paraptotic cell death induced by Cu(CQ) does not require nor involve caspases, giving an indication for the current clinical assessment of clioquinol as an antineoplastic agent.
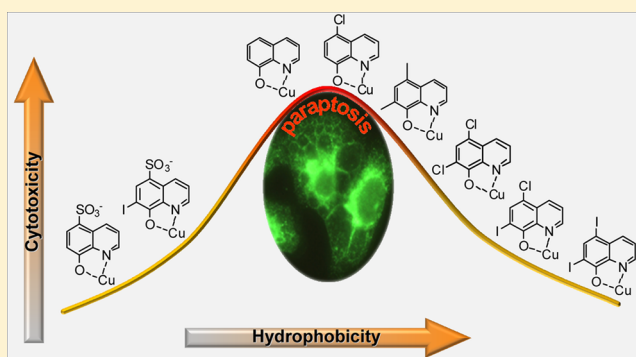
INTRODUCTION

Several types of programmed cell death (PCD) have been reported in the literature.[1] Caspase-dependent apoptosis is the most common type of PCD through which normal and tumor cells die in an organized manner, both during tissue development and under conditions of stress, such as chemo-therapeutic treatment.[2] From a morphological point of view, apoptosis is manifested with cell shrinkage, chromatin condensation, and the appearance of apoptotic bodies containing nuclear fragments. The apoptotic process can be activated either by extracellular ligands through transmembrane death receptors (extrinsic pathway) or as a consequence of cellular injury that ultimately leads to mitochondrial membrane permeabilization and release of cytochrome *c* (intrinsic pathway). The complex biochemical machinery activated during the cell death process usually promotes the activation of caspase-3, which dismantles cellular architecture and leads to cell death.[3,4] However, caspase-independent apoptosis has also been documented.[1] Caspase-independent apoptotic cell death usually comprises the translocation of endonucleases (ENDOG) and/or apoptosis-inducing factor (AIF) from the mitochondria to the nucleus.[5,6] The extensive stress on the endoplasmic reticulum (ER) caused by the accumulation of unfolded proteins in its lumen can trigger the apoptotic pathway. In the presence of this stress, cells activate the

unfolded protein response (UPR) and inhibit protein synthesis in an effort to relieve the ER from excessive protein overload. If the stress persists, the expression of the transcription factor CHOP (CCAAT-enhancer-binding protein homologous pro-tein) increases, initiating the apoptotic cascade.[7,8]

We have recently reported that an elevated intracellular copper concentration activates the UPR, either by inhibiting the proteasome, which is responsible for the degradation of misfolded proteins, or by promoting protein misfolding.[9] This latter process is most likely due to the redox ability of the metal ion because intracellular copper accumulation is accompanied by a decrease of the reduced form of glutathione (GSH) and an increase of its oxidized form (GSSG).[10] Interestingly, the copper-dependent UPR does not lead to apoptosis because of the inhibition of caspase-3 by the metal, but rather an alternative type of PCD characterized by extensive cytoplasmic vacuolization, which is the morphological hallmark of para-ptosis, is induced.[9] Other examples of caspase-3-independent, paraptosis-like cell death associated with ER stress and UPR upon treatment of lymphoma cells with cannabinoids were recently reported.[11] In another report, the use of curcumin induced paraptosis in malignant breast cell lines.[12,13] These

findings provide further evidence that paraptosis can be activated in different cell lines with structurally and functionally unrelated compounds and may serve as an alternative, drug-induced death pathway for cancer and normal cells unable to undergo apoptosis.

Copper is an essential metal ion involved in several highly conserved biochemical processes. Its oxidation state shifts from +2 to +1 upon internalization because of the reducing intracellular environment. The metal is taken up by the cell through the copper transporter hCTR1,[14,15] and a number of chaperones deliver it to its intracellular destinations, i.e., Cu−Zn superoxide dismutase and cytochrome *c* oxidase. A mild intracellular excess of copper can normally be balanced by the cells through an increased expression of metallothioneins or through the activation of specific pumps, such as ATP7A and ATP7B,[16−18] whereas high copper concentrations cause the activation of the UPR, as described above. For this reason, despite its essential role in living cells, copper has been frequently employed in the preparation of cytotoxic complexes. In many instances, the choice of Cu(II)-based compounds as cytotoxic agents originates from the overproduction of reactive oxygen species (ROS) driven by the metal. Alternatively, copper-binding agents have been employed for their ability to direct the toxicity of the metal toward specific intracellular targets.[19,20]

In cultured cells, the internalization of copper complexes does not usually involve the hCTR1 copper-specific transporter but rather occurs primarily via passive diffusion.[9,21] For this reason, the chemical features of the ligand appear to be the main determinants of the activity of the complex because they may (i) modulate its permeability through the cell membranes by virtue of its lipophilic character, (ii) stabilize a specific redox state of the metal, (iii) drive the complex to specific cellular targets, and (iv) exhibit an intrinsic cytotoxic activity when dissociated from the metal. 8-Hydroxyquinoline (8-HQ) derivatives are planar, N,O-donating ligands that have a high affinity for Cu(II) (Figure 1). Particular interest has recently been dedicated to 5-Cl-7-I-8-HQ (clioquinol, CQ) because CQ

was already recognized as an antiparasitic drug, even though its use was discontinued in some countries because of the occurrence of subacute myelo-optic neuropathy.[22] CQ is currently used as an antifungal and antibacterial in the commercial cream Vioform. In mice, CQ proved to be able to inhibit the accumulation of β amyloid (Aβ) in the brain and to mobilize the Aβ from existing deposits,[23] which are of great relevance for treatments of Alzheimer disease.[24,25] The CQ-related compound PBT2[26] recently underwent phase II clinical trials as an anti-Alzheimer compound.[27] Moreover, CQ has entered phase I clinical trials for the treatment of relapsed or refractory hematological malignancies (NCT00963495).

In previous research, we have shown that nitrogen donor ligands behave as copper ionophores in cancer cells, thus leading to a toxic accumulation of the metal, which eventually triggers paraptotic cell death.[9,10,28] The goal of this project is to investigate whether nonapoptotic programmed cell death is activated in tumor cell lines by the combined treatment with copper and 8-HQ analogues, with a particular focus on the copper ionophore CQ.[29,30]

■ RESULTS

Molecular Structures and Stability Constants of Cu(II) Complexes with 8-HQ Derivatives. The Cu(II) complexes can be prepared by mixing $CuCl_2 \cdot 2H_2O$ and the corresponding ligands in the 1:1 or 1:2 molar ratio as specified in the Experimental Section. Complexes of formula $[Cu(L)(H_2O)_2]$ are obtained with the $5\text{-}SO_3\text{-}8\text{-}HQ$ and $5\text{-}SO_3\text{-}7\text{-}I\text{-}8\text{-}HQ$ ligands, whereas the remaining ligands give rise to complexes of $[Cu(L)_2]$ general formula (Figure 1). Given the different lipophilic properties of the ligands, different solvents were employed to prepare solutions of the ligands, whereas $CuCl_2 \cdot 2H_2O$ was dissolved in methanol. The $[Cu(L)(H_2O)_2]$ or $[Cu(L)_2]$ complexes readily precipitated from the reaction mixtures as brown or green powders. These compounds are usually insoluble in aqueous media and in common organic solvents and are poorly soluble in DMSO. For this reason, the biological tests were performed by mixing $CuCl_2 \cdot 2H_2O$ and the corresponding ligands directly into the cell culture media at a 1:1 molar ratio. The final concentration of the complex for the biological tests was in the $1-30$ μM range such that it did not precipitate in the medium. On the basis of our determined stability constants for 8-HQ and $5\text{-}SO_3\text{-}8\text{-}HQ$ (see below) in this range of concentrations, we expect that in aqueous media and with no competitor ligands, 40−50% of the total Cu(II) forms $[Cu(L)]$ while the remaining 50−60% is present as $[Cu(L)_2]$ and "free" Cu^{2+} ions (25−30% each) (Supporting Information, Figure S1).

8-HQ and its derivatives are characterized by the presence of a N,O-binding system that is suitable for interacting strongly with Cu(II) ions. Figure 1 depicts the general molecular structures of the complexes of formula $[Cu(5\text{-}R\text{-}7\text{-}R'\text{-}8\text{-}HQ)_2]$. The presence of the $-SO_3^-$ group leads to the formation of complexes in which the metal/ligand ratio is 1:1 because of the involvement of the sulfonate moiety in metal coordination.[31−33] When R and R' are halogen or alkyl substituents, the metal/ligand ratio becomes 1:2 and the ligands are arranged in a trans geometry, with the nitrogen and oxygen atoms on the opposite side with respect to the metal center. The molecular structures of $[Cu(8\text{-}HQ)_2]$[34] and $[Cu(CQ)_2]$[35] were previously reported, whereas that of $[Cu(5,7\text{-}Me\text{-}8\text{-}HQ)_2]$ is reported in Figure 1B and in the Supporting Information, Figure S5.
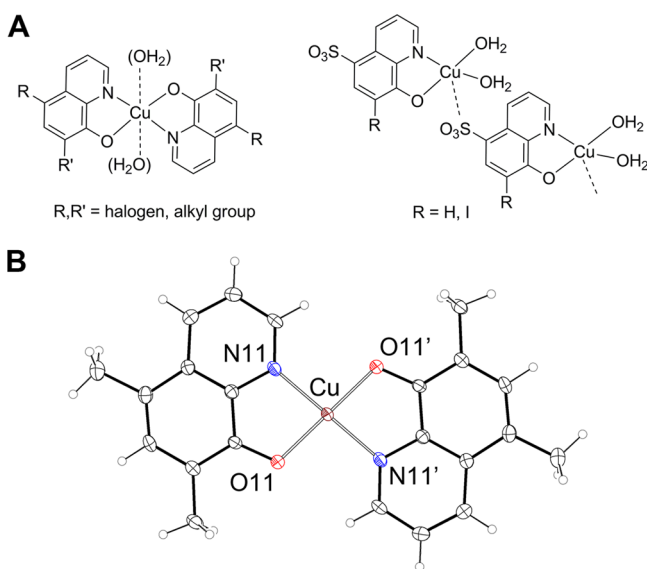

Figure 1. (A) Molecular structures of Cu(II) complexes with 8-HQ derivatives. (B) ORTEP diagram of the X-ray molecular structure of $[Cu(5,7\text{-}Me\text{-}8\text{-}HQ)_2]$, symmetry code = $-x$, $1 - y$, $-z$.
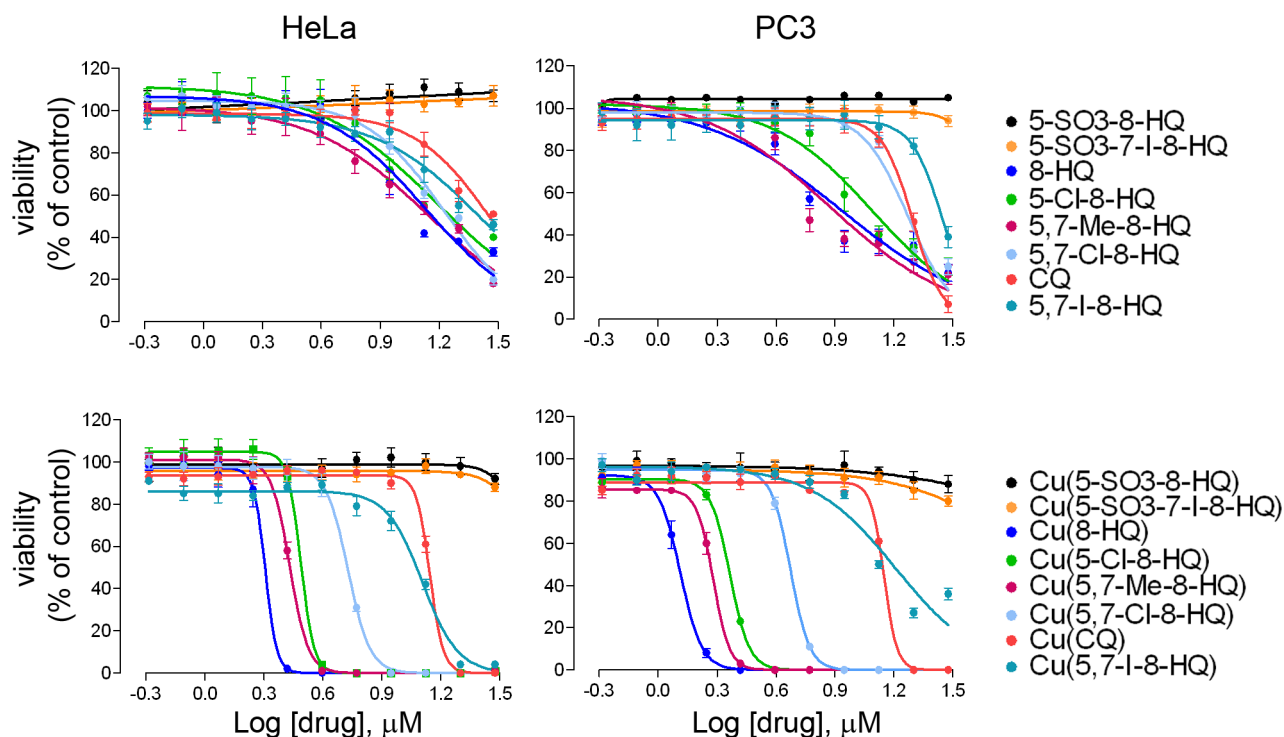
Figure 2. Dose−response curves for ligands and copper complexes in HeLa and PC3 cells. HeLa and PC3 cells were incubated for 48 h with different concentrations of ligands (upper panels) or copper complexes (lower panels). Cell viability after treatment was assessed using the resazurin method. The data presented are the mean ± SEM of three independent experiments, each performed in triplicate. Error bars are visible when larger than the symbols.

The stability constants of $[Cu(5\text{-}SO_3\text{-}8\text{-}HQ)(H_2O)_2]$ and $[Cu(8\text{-}HQ)_2]$ were determined by potentiometry in a 1:1 DMSO/water (w/w) solution. The Cu(II) complexes with these ligands were remarkably stable, with log β_1 and log β_2 values of about 11.5 and 22.5 for both 8-HQ and 5-SO_3-8-HQ (see Supporting Information, Table S1). Previous studies reported the stability of these ligands in water,[36] although most studies were performed in water/organic mixtures such as alcohol[37] or water/dioxane mixtures[38,39] to address solubility problems. These studies reported formation constants that fall in the range log β_1 of 11−14 and log β_2 of 22−25.[40,41] In this study, we used a DMSO/water mixture as an attempt to increase the solubility of the various species in order to determine the stability constants in homogeneous conditions. Unfortunately, the poor solubility of the remaining ligands (or their complexes) in this mixture made it difficult to measure the stability constants for the other complexes. Our values fall within the range determined in different solvents, showing that the presence of DMSO does not significantly affect the stability of the complexes. Moreover, the similarity of the values of log β for 5-SO_3-8-HQ and 8-HQ suggests that any interaction between the $[Cu(L)]$ species and a ligand molecule via the sulfonate group (as found in the solid state) is negligible in solution. The influence exerted by the substituents in the 5 and 7 positions on the hydroxyquinoline moiety is also expected to have minimal steric influence on the geometry of the Cu(II) complexes and therefore on their stability due to the positioning of these groups at the exterior of the coordination site (see Figure 1).

Interestingly, the $[Cu(L)_2]$ compounds can precipitate out as solids when using the 1:1 molar ratio (except those with the 5-SO_3-8-HQ and 5-SO_3-7-I-8-HQ ligands that form complexes with Cu/L 1:1 stoichiometry). This behavior can be accounted
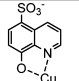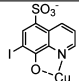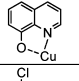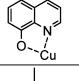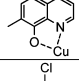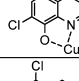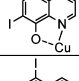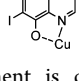
for by their log β values. In fact, the stability constants of the coordination of Cu(II) with the first ligand (giving $[Cu(L)]$, log β_1) and the second ligand ($[Cu(L)_2]$, log K_2 = log β_2 − log β_1) are approximately the same. As a result, the amount of $[Cu(L)_2]$ in solution for a HL/Cu(II) ratio of 1 is quite high (∼20% total copper for both ligands), likely leading to the precipitation of this neutral complex from the solution (see discussion in the Supporting Information). This finding is in agreement with the poor solubility of the $[Cu(L)_2]$ complex with 8-HQ (∼10^{-6} M),[36] which precipitates out of solution at a HL/Cu(II) ratio greater than 1.2, even at pH ≈ 4.5 and C_{Cu} ≈ 10^{-4} M.

The stability of the complexes $[Cu(8\text{-}HQ)_2]$ and $[Cu(5\text{-}SO_3\text{-}8\text{-}HQ)(H_2O)_2]$ in the presence of human serum albumin (HSA) was evaluated by means of circular dichroism (Figure S4).[42] The concentration of albumin in the samples was 85 μM, close to that used in the biological experiments (around 60 μM). The CD spectra in the presence of CuCl_2 (control), $[Cu(8\text{-}HQ)_2]$, and $[Cu(5\text{-}SO_3\text{-}8\text{-}HQ)(H_2O)_2]$ show a Cotton effect in the range 450−650 nm related to the Cu(II) d−d transitions and indicative of the coordination of Cu(II) to the high affinity binding site at the N-terminus of the protein. By comparison of the CuCl_2/HSA, $[Cu(8\text{-}HQ)_2]$/HSA, and $[Cu(5\text{-}SO_3\text{-}8\text{-}HQ)(H_2O)_2]$/HSA systems, a lower Cotton effect is observed in the presence of hydroxyquinoline ligands, indicating that albumin is not able to completely displace the metal from the ligands. Overall, these data demonstrate that the complexes are stable to a significant extent even in the presence of albumin.

Effects of the Ligands and Complexes on HeLa and PC3 Cell Viability. The cytotoxic potential of the ligands was evaluated in two human tumor cell lines derived from cervical carcinoma, HeLa, and prostatic adenocarcinoma, PC3. As

shown in Figure 2 (upper panels), all ligands present cytotoxic activity except for 5-SO$_3$-8-HQ and 5-SO$_3$-7-I-8-HQ, which are almost ineffective on both cell lines up to the maximum concentration employed (30 μM). For six out of the eight 8-HQ derivatives, adding an equimolar amount of CuCl$_2$ dramatically increases the effect of the ligands in both HeLa and PC3 cells (Figure 2, lower panels), decreasing the IC$_{50}$ values of the active ligands in both cell models. The addition of copper shifts the range of ligand IC$_{50}$ from 13.5−25.2 to 1.9−12.8 μM and from 8.6−25.7 to 1.3−16.2 μM in HeLa and PC3, respectively (Table 1 and Table S3, for comparison).

Table 1. Molecular Structures of the Copper Complexes[a] and the IC$_{50}$ (μM) Values[b] in HeLa and PC3 Human Tumor Cell Lines

Complex	Structure	Ligand LogP	IC$_{50}$ (HeLa)	IC$_{50}$ (PC3)
Cu(5-SO$_3$-8-HQ)		-0.21	n.d.	n.d.
Cu(5-SO$_3$-7-I-8-HQ)		0.70	n.d.	n.d.
Cu(8-HQ)		1.84	1.9	1.3
Cu(5-Cl-8-HQ)		2.58	3.1	2.3
Cu(5,7-Me-8-HQ)		2.66	2.7	1.9
Cu(5,7-Cl-8-HQ)		3.22	5.3	4.7
Cu(CQ)		3.50	8.9	9.0
Cu(5,7-I-8-HQ)		3.75	12.8	16.2

[a]Only the CuL fragment is depicted. [b]The cytotoxic activity is measured for mixtures composed of CuCl$_2$ and hydroxyquinoline derivatives in a 1:1 molar ratio.

Interestingly, a nonlinear correlation between the lipophilic character of the ligand, which is modulated by the peripheral functional groups, and the cytotoxic activity of the corresponding copper complex was found. When the ligands are ranked by increasing lipophilic character, i.e., with increasing log P values, the activities of the corresponding complexes describe a bell-shaped curve (Figure 3). According to this relationship, the highest cytotoxic activity is expected to be exhibited by ligands with intermediate log P values, namely, between 1.5 and 3.

Although the complex Cu(CQ) is significantly less active than Cu(8-HQ) in both cell lines, we decided to further investigate its biological behavior, given the known and documented use of clioquinol as a drug[43] and the recent attention paid to its anticancer potential in vitro and in vivo.[30,44,45]

To evaluate the effect of the drug and its copper complex in nonmalignant cells, their effects have been tested in normal human cells (HUVEC, human umbilical vein endothelial cell; HF, human fibroblast). The vascular endothelium is one of the first tissues that drugs come in contact with during the administration of chemotherapy. The study of the effects of the two compounds on vascular endothelial cells is therefore of peculiar interest, given their potential application to clinical practice. Because endothelial cells are routinely grown in the presence of 20% FBS, for these specific experiments, the serum concentration was raised from 10% to 20% for all cell types. In HUVEC, the cytotoxic activity of the ligand remains negligible at all concentrations tested, whereas the corresponding complex exhibits an IC$_{50}$ of 25.2 μM. Notably, the presence of higher serum levels diminishes the cytotoxic effect of Cu(CQ) in tumor cell lines, with the IC$_{50}$ values of Cu(CQ) being 14.8 and 10.9 μM in HeLa and PC3, respectively (Figure 4). This effect is likely due to the copper binding activity of the serum components. Indeed, when Cu(CQ) is tested under low serum conditions (10%), its cytotoxic activity appears to be considerably increased in all cell models, although with approximately the same differential efficacy in normal and tumor cells (Figure S7).

As far as normal human fibroblasts are concerned, concentrations up to 8.9 μM of the copper complex do not exert any significant effect, either on cell number or on lactate dehydrogenase (LDH) release (Figure S8). Beyond this concentration, LDH release significantly increases and cell number concomitantly decreases, indicating a cytotoxic effect. However, a complete cell loss cannot be detected even at the
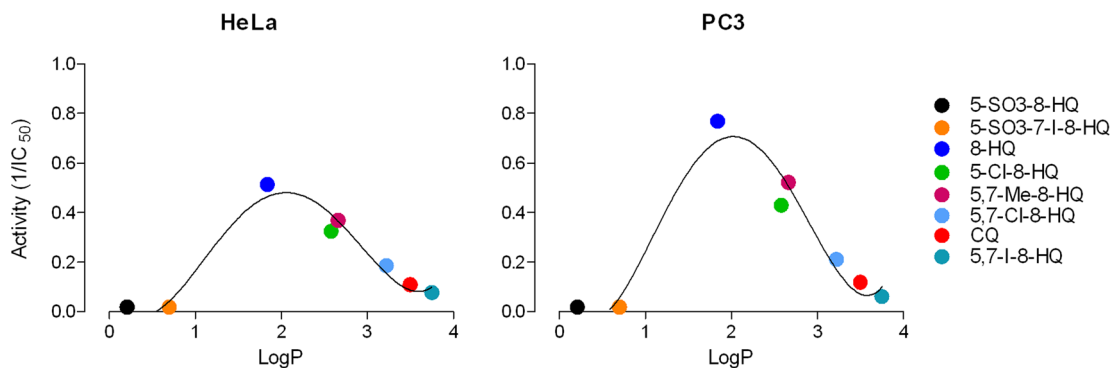

Figure 3. Correlation between cytotoxic activity of copper complexes and ligand log P. The activities of the copper complexes, calculated as the inverse of IC$_{50}$ in HeLa and PC3 cells, were matched with corresponding ligand log P values. The curves were extrapolated with the GraphPad Prism software.
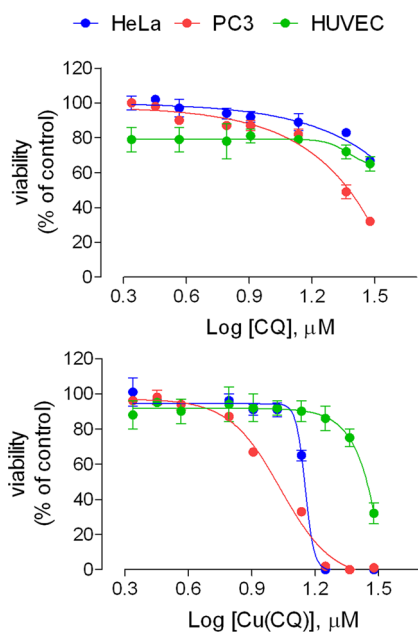
Figure 4. Comparison of dose−response curves of CQ and Cu(CQ) in HeLa, PC3, and HUVEC cells. Different concentrations of CQ and Cu(CQ) were tested for 48 h on the cells in the presence of 20% FBS. After the treatment, viability was assessed using the resazurin method. The data presented are the mean ± SEM of three independent experiments, each performed in quadruplicate. Error bars are visible when larger than the symbols.

maximum concentration tested (30 μM), suggesting that a fraction of the cell culture is highly resistant to Cu(CQ).

Characterization of Cu(CQ)-Dependent Cytotoxicity. It has been reported that the cytotoxicity induced by clioquinol is maximally increased by the presence of copper and is associated with caspase activation.[46] To assess whether the metal and/or caspases are required for the Cu(CQ) cytotoxic effect, HeLa and PC3 cells were incubated with increasing doses of Cu(CQ) in the presence of a high affine extracellular copper chelator, ammonium tetrathiomolybdate (TM),[47,48] or of a cell-permeable pan-caspase inhibitor, z-VAD-FMK.

As shown in Figure 5A, the addition of TM dramatically reduces the cytotoxic effect of the complex: the IC$_{50}$ of Cu(CQ) moves from 9.0 and 8.9 μM to 24.5 and 21.5 μM in HeLa and PC3, respectively, and the dose−response profile of the complex in the presence of TM becomes similar to that of the CQ ligand alone. Interestingly, higher doses of TM have a moderately toxic effect on HeLa cells, as shown by the dose−response curve of Cu(CQ) in the presence of 40 μM TM (Figure S9). On the contrary, curves obtained upon treatment of HeLa and PC3 cells with the complex in the absence and presence of z-VAD-FMK are comparable, suggesting that copper, not caspases, is essential for the Cu(CQ) mechanism of action.

To directly assess the effect of Cu(CQ) on cellular copper homeostasis, the intracellular content of the metal has been measured by means of ICP-AES in cells treated for different times with 14 μM Cu(CQ). A marked time-dependent accumulation of copper can be observed in both cell models (Figure 5B), with the maximum effect being evident after 6 h, when copper content is 70- and 50-fold increased in HeLa and PC3 cells, respectively, with respect to control (untreated cells). As expected, the simultaneous incubation of the cells with
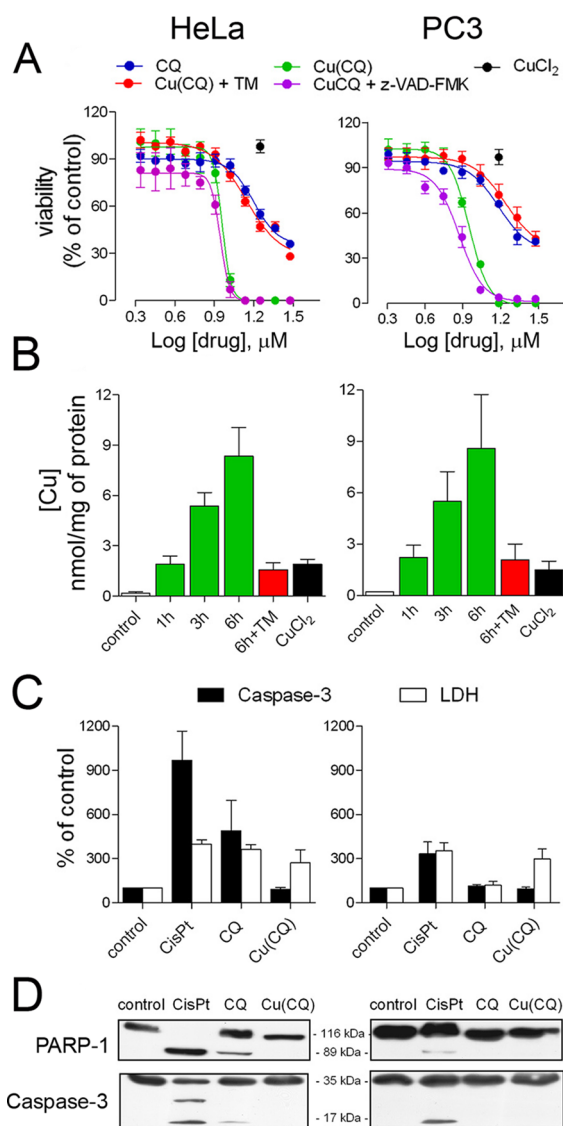

Figure 5. Characterization of Cu(CQ)-dependent cytotoxicity. (A) HeLa and PC3 cells were treated for 48 h with different concentrations of CQ or Cu(CQ), either in the absence or presence of 20 μM TM or 50 μM z-VAD-FMK or with 14 μM CuCl$_2$. Cell viability was assayed using the resazurin method. The data presented are the mean ± SEM of three independent experiments, each performed in quadruplicate. Error bars are visible when larger than the symbols. (B) HeLa and PC3 cells were treated for the indicated times with 14 μM Cu(CQ) in the absence or presence of 20 μM ammonium tetrathiomolybdate (TM) or with 14 μM CuCl$_2$. The intracellular copper content was measured by means of ICP-AES, as described in the Experimental Section. The bars are the mean ± SEM of two independent measurements in two different experiments. (C) HeLa and PC3 cells were untreated or treated with cisplatin (CisPt, 20 and 50 μM, respectively), 50 μM CQ, or 14 μM Cu(CQ). After 18 h, caspase-3 activity and LDH release were assayed in cell lysates and in the incubation medium, respectively. The data are the mean ± SEM of four independent experiments. (D) The levels of cleaved PARP-1 and caspase-3 proteins were assessed in cell lysates of both HeLa and PC3 cells, either untreated or treated for 18 h with 20 and 50 μM CisPt, respectively, 50 μM CQ, or 14 μM Cu(CQ). The experiment was repeated twice with comparable results. Representative Western blots are shown.

Cu(CQ) and 20 μM TM lowers the intracellular copper content to values comparable to those of untreated cells (Figure 5B), thus confirming the ionophoric properties of

clioquinol. Consistently with the absence of effects on HeLa and PC3 cells viability (Figure 5A), treatment with 14 μM CuCl$_2$ only causes a modest increase of intracellular copper content, as compared to that occurring upon incubation with the same concentration of Cu(CQ) (Figure 5B).

Data obtained from the dose–response experiment performed in the presence of the caspase inhibitor excluded the possibility of substantial involvement of caspases in mediating the cytotoxic effect of Cu(CQ) but not in their eventual activation. We have therefore addressed the activity of caspase-3, the final executor in caspase-dependent apoptosis, in Cu(CQ)-treated cells. Caspase-3 is not activated in HeLa and PC3 cells treated with the complex at the IC$_{75}$ (14 μM), a concentration at which the culture is undergoing substantial cell death as shown by the marked release of LDH, a marker of membrane rupture (Figure 5C). Conversely, the activation of caspase-3 is readily detectable upon treatment of HeLa cells with CQ at the maximum concentration tested (50 μM). Consistent with the results obtained by means of the biochemical assay, Western blot analysis demonstrates the cleavage of caspase-3 in HeLa cells treated with 50 μM CQ but not in HeLa and PC3 cells incubated with Cu(CQ) (Figure 5D).

During the apoptotic process, poly ADP-ribose polymerase-1 (PARP-1), a nuclear protein involved in the repair of DNA breaks, is cleaved by caspases and inactivated to spare energy in favor of the apoptotic cell death.[49,50] In Figure 5D, it is shown that PARP-1 is extensively cleaved in both HeLa and PC3 cells upon treatment with the apoptosis inducer cisplatin, moderately cleaved in 50 μM CQ-treated HeLa cells, and not cleaved at detectable levels under any other conditions. Altogether, these results exclude the possibility of activation of caspases and more specifically of caspase-3 during the cell death process induced by Cu(CQ) in HeLa and PC3 cells. Conversely, a caspase-3 dependent apoptotic pathway appears to be involved in clioquinol driven cytotoxicity, since the pan-caspase inhibitor z-VAD-FMK partially protects HeLa cells from the cytotoxic effect of CQ on both morphological (Figure 6A) and biochemical (Figure 6B) grounds.

Finally, to further explore the molecular mechanisms underlying Cu(CQ) cytotoxicity, the subcellular localization of apoptosis-inducing factor (AIF) has been addressed in HeLa cells by means of confocal microscopy. As shown in Figure S10, a clear-cut nuclear staining of AIF is readily detectable upon treatment with staurosporin, a toxin known to induce the nuclear translocation of the factor from mitochondria.[51] At variance, CQ and Cu(CQ)-treated cells do not show any appreciable nuclear staining, since the signal remains typically cytoplasmic as in control, untreated cells.

■ DISCUSSION

We have recently shown that different classes of nitrogen-donor ligands behave as copper ionophores and thus cause a toxic accumulation of the metal in cancer cells, which ultimately undergo a peculiar type of UPR-dependent, nonapoptotic cell death.[9] In the present study, we address the structure–activity relationship of copper complexes with 8-HQ derivatives, as well as their ability to trigger cell death. 8-HQ analogues are ligands with a high affinity for copper that they bind through a N,O-donor moiety.[30,46,52] The stability constants of the corresponding complexes, which describe the interaction between the ligands and the Cu(II) ions, are orders of magnitude higher than those exhibited by endogenous Cu(II)-complexing
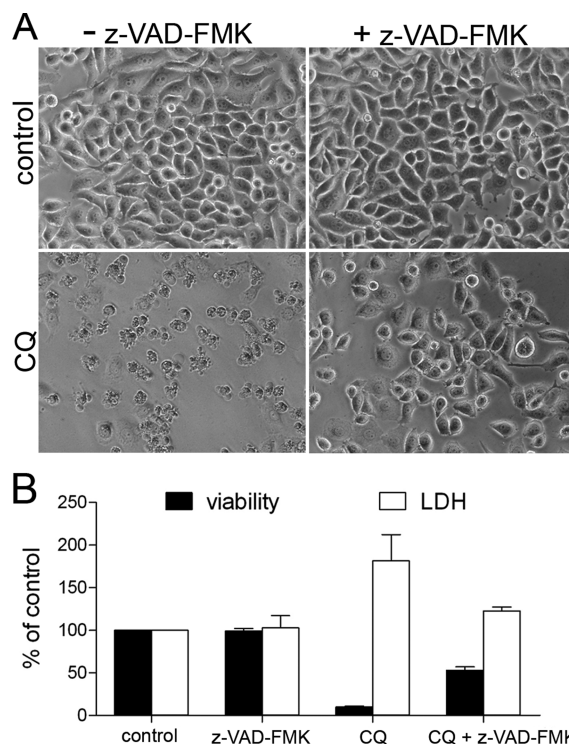

Figure 6. Role of caspases in CQ-dependent cytotoxicity. HeLa cells were treated with 50 μM CQ, both in the absence and in the presence of 50 μM z-VAD-FMK for 18 h (control is untreated cells). (A) Phase contrast images of representative microscopic fields (200×) are shown. (B) Cell viability was assayed with the resazurin method, and LDH release was determined in the incubation medium. Data are the mean ± SD of three replicates within a representative experiment.

ligands, i.e., amino acids,[40] and thus suggest a moderate/high stability of these complexes with 1:1 and 1:2 Cu/L stoichiometry. Nevertheless, it is generally accepted that once a Cu(II) complex enters the cells, the reducing environment favors the Cu(II) → Cu(I) reduction, causing a decrease in ligand affinity for the metal. The presence of other highly affine Cu(I) ligands within the cell most likely results in the displacement of the ligand from the ion.[53,54]

The majority of cytotoxic drugs must enter the cell to express their cytotoxic potential. Entry may occur through active transport, as proposed for the internalization of cisplatin by the copper transporter hCTR1[55,56] or by passive diffusion across the plasma membrane. In the latter case, the drug must be endowed with the appropriate lipophilicity so that it can cross the cell membrane and reach the threshold intracellular concentration. An overly lipophilic compound would accumulate in the membrane, while a large hydrophilicity would prevent interactions with the lipid bilayer. Consistent with the results described in this study, the literature reports several examples of homologous series of species whose cytotoxic activity correlates with lipophilicity.[57−59] Among the 8-HQ derivatives examined, the most hydrophilic ligands 5-SO3-8-HQ and 5-SO3-7-I-8-HQ do not display any cytotoxic activity when complexed with copper, whereas the most active complexes are those with ligands of intermediate lipophilicity, namely, 8-HQ, 5,7-Me-8-HQ, and 5-Cl-8-HQ.

Although copper forms the most active complex with 8-HQ, we have decided to focus on the effects of CQ–copper complex. CQ is a known antibiotic drug,[60] has been extensively investigated as an anti-Alzheimer compound,[24,25,61] and has
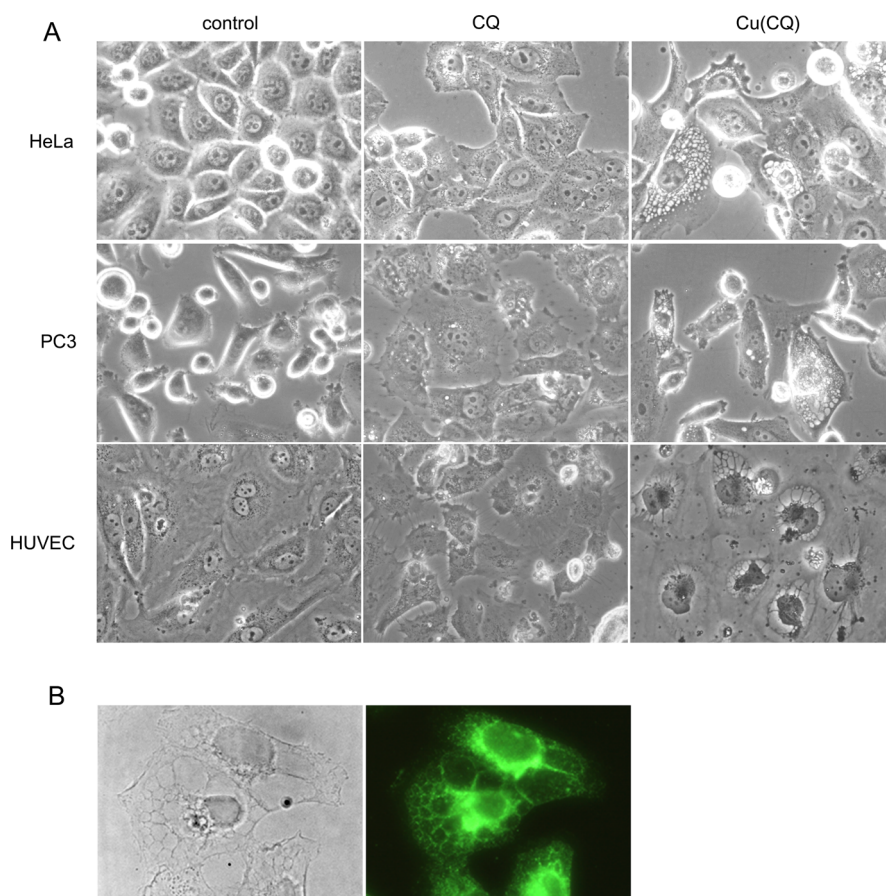
Figure 7. Cu(CQ)-induced cytoplasmic vacuolization. (A) HeLa, PC3, and HUVEC cells were grown with 10% FBS and treated with 50 μM CQ and 8 μM (HeLa and PC3) or 15 μM (HUVEC) Cu(CQ) for 18 h. Control is untreated cells. Phase contrast images of representative microscopic fields (400×) are shown. (B) HeLa cells were treated with 8 μM Cu(CQ) for 18 h, and the immunostaining of endoplasmic reticulum was performed with calnexin, as described in the Experimental Section. The phase contrast (left) and the immunostaining (right) images of the same representative microscopic field (1000×) are shown.

ionophoric properties that have been previously investigated with copper and zinc.[29,30] It has been demonstrated that the CQ−copper complex cytotoxicity in breast cancer cells is due specifically to the metal binding and transport ability of clioquinol.[62] Consistently, we show here that the simultaneous addition of CuCl$_2$ to CQ-treated HeLa and PC3 cells results in a time-dependent increase of intracellular copper in both cell models (Figure 5B). Moreover, the incubation of the cells in the presence of the cell-impermeable copper chelator ammonium tetrathiomolybdate (TM)[47,48] hinders copper accumulation (Figure 5A) and protects both HeLa and PC3 cells from the cytotoxic effect of Cu(CQ) (Figure 5B). Interestingly, when the concentration of TM is raised to 40 μM, it selectively affects the growth of HeLa cells (Figure S9), which is in agreement with the anticancer mechanism of TM. It has been proposed that TM, by virtue of its ability to sequester copper, directly affects malignant cell growth[63] and acts as an antiangiogenic factor impairing vascular endothelial cells functions.[64]

The anticancer activity of CQ alone[30] or in combination with Zn(II) and Cu(II) ions was recently reported to activate a caspase-3-dependent cell death process[65] and more specifically to activate the apoptotic pathway in breast cancer KCL2 cells.[66] On the contrary, our results show that Cu(CQ)-dependent cytotoxicity does not require the activation of caspases in HeLa and PC3 cells because the pan-caspase inhibitor z-VAD-FMK

fails to rescue cell death (Figure 5A). Moreover, while a classical proapoptotic stimulus, i.e., cisplatin, activates caspase-3 in HeLa and PC3, cytotoxic concentrations of Cu(CQ) do not (Figure 5C,D). Intriguingly, the treatment of HeLa cells with high concentrations of CQ alone moderately activates caspase-3 (Figure 5C) and the addition of the caspase inhibitor z-VAD-FMK partially rescues HeLa cells from the cytotoxic effect observed upon treatment with high doses of CQ (Figure 6), thus indicating that the mechanism of action of the ligand substantially differs from that of the complex, at least in this cellular model.

One of the substrates of caspase-3 is poly ADP-ribose polymerase-1 (PARP-1), an enzyme that signals DNA breaks and recruits the DNA repair complex. Because PARP-1 activation is energy consuming, cells committed to apoptotic death cleave and inactivate PARP-1. On the other hand, it was recently shown that the activation of PARP-1 is one of the key steps of programmed necrosis.[67,68] In our cell models, PARP-1 is cleaved upon cisplatin-induced apoptosis (Figure 5D), but it is not cleaved upon Cu(CQ) treatment, confirming the nonapoptotic nature of the death process triggered by the complex. A further independent evidence confirming that the Cu(CQ)-dependent cell death is distinct and distinguishable from apoptosis comes from the lack of translocation of apoptosis inducing factor (AIF) from mitochondria to the nucleus upon treatment with the copper complex (Figure S10).

Although the enzymes responsible for the paraptosis execution remain to be identified, the morphology of dying cells can nonetheless provide useful hints to the identification of the mechanisms involved in this type of cell death. An increasing number of reports refer to paraptosis as non-apoptotic cell death characterized by a massive cytoplasmic vacuolization due to endoplasmic reticulum swelling. In particular, these features have been frequently observed upon treatment with copper-based compounds.[9,28,69,70] Consistently, HeLa, PC3, and HUVEC cells treated with cytotoxic doses of Cu(CQ) display the prototypical traits of paraptosis (Figure 7).

These results confirm the ionophoric nature of 8-HQ derivatives for copper, pinpoint the ligand hydrophobicity as a determinant of the activity of the complex, and demonstrate that the ligand dependent copper accumulation triggers a nonapoptotic cell death, morphologically defined as paraptosis, that does not activate or depend on caspase activity.

Altogether these findings may support the combined use of CQ and copper for the treatment of tumors characterized by innate or acquired apoptosis resistant phenotype. On the contrary the combination of clioquinol, copper, and proapoptotic agent may be evaluated carefully in order to avoid conflicting effects on caspase activation. The differential cytotoxicity of Cu(CQ) in tumor and normal cells also supports its potential chemotherapeutic application in clinical practice, with reasonably minor adverse side effects.

■ EXPERIMENTAL SECTION

All reagents and solvents were commercially available. Infrared spectra were recorded from 4000 to 700 cm^{-1} on a Perkin-Elmer FT-IR Nexus spectrometer equipped with a Thermo-Nicolet microscope. Compound purity was assessed by means of combustion analysis (Carlo Erba EA 1108 automated analyzer) with a confirming purity of ≥95% for all copper complexes.

Synthesis of [Cu(5-SO$_3$-8-HQ)(H$_2$O)$_2$]. A pale green solution of CuCl$_2$·2H$_2$O (94 mg, 0.55 mmol) dissolved in methanol (5 mL) was added to a solution of 8-hydroxyquinoline-5-sulfonic acid (125 mg, 0.56 mmol) in 10 mL of methanol/water (1/1), and then the mixture was stirred for 30 min. A green solid precipitated. The solvent was concentrated under vacuum, and the solid was filtered and vacuum-dried (156 mg, yield 88%). IR (cm^{-1}): 454s, 547m, 624m, 706m, 778w, 1024m, 1139s, 1320w, 1369w, 1490m, 1572w, 2847w broad, 3091w sharp, 3165m broad. Anal. Calcd for C$_9$H$_9$CuNO$_6$S (322.78): C, 33.49; H, 2.81; N, 4.34. Found: C, 33.17; H, 2.59; N, 4.16%.

Synthesis of [Cu(5-SO$_3$-7-I-8-HQ)(H$_2$O)$_2$]. A pale green solution of CuCl$_2$·2H$_2$O (61 mg, 0.35 mmol) dissolved in methanol (5 mL) was added to a pale yellow solution of 8-hydroxy-7-iodo-5-quinolinesulfonic acid (123 mg, 0.35 mmol) in 30 mL of methanol/water (8/2), and the mixture was stirred for 30 min. A green solid precipitated. The solvent was concentrated under vacuum, and the solid was filtered and vacuum-dried (131 mg, yield 83%). IR (cm^{-1}): 591s, 728m, 816m, 1035s, 1167s, 1380m, 1484m, 1556w, 1626w, 3073w, 3195w, 3343m broad, 3526m sharp. Anal. Calcd for C$_9$H$_8$CuINO$_6$S (448.68): C, 24.09; H, 1.80; N, 3.12. Found: C, 23.81; H, 1.97; N, 3.33%.

Synthesis of [Cu(8-HQ)$_2$]. A pale green solution of CuCl$_2$·2H$_2$O (147 mg, 0.86 mmol) dissolved in methanol (5 mL) was added to a yellow solution of 8-hydroxyquinoline (250 mg, 1.72 mmol) in 20 mL of methanol, and a brown solid precipitated immediately. After 30 min of stirring, the solid was filtered and vacuum-dried (233 mg, yield 77%). IR (cm^{-1}): 504m, 635w, 739s, 821s, 1106s, 1265m, 1315s, 1375s, 1495s, 1578m, 3057w. Anal. Calcd for C$_{18}$H$_{14}$CuN$_2$O$_2$ (351.85): C, 61.44; H, 3.44; N, 7.96. Found: C, 61.27; H, 3.57; N, 7.71%.

Synthesis of [Cu(5-Cl-8-HQ)$_2$]. A pale green solution of CuCl$_2$·2H$_2$O (119 mg, 0.69 mmol) dissolved in methanol (5 mL) was added to a yellow solution of 5-chloro-8-hydroxyquinoline (250

mg, 1.39 mmol) in 20 mL of methanol, and a brown solid precipitated immediately. After 30 min of stirring, the solid was filtered and vacuum-dried (196 mg, yield 68%). IR (cm^{-1}): 428m, 646m, 745s, 772m, 964m, 1064m, 1084m, 1309s, 1364s, 1463m, 1583m, 3063w. Anal. Calcd for C$_{18}$H$_{10}$CuCl$_2$N$_2$O$_2$ (420.74): C, 51.38; H, 2.40; N, 6.66. Found: C, 51.61; H, 2.58; N, 6.29%.

Synthesis of [Cu(5-Me-7-Me-8-HQ)$_2$]. A pale green solution of CuCl$_2$·2H$_2$O (123 mg, 0.72 mmol) dissolved in methanol (5 mL) was added to a pale pink solution of 5,7-dimethyl-8-hydroxyquinoline (250 mg, 1.44 mmol) in 20 mL of methanol, and a green solid precipitated immediately. After 30 min of stirring, the solid was filtered and vacuum-dried (221 mg, yield 76%). Suitable crystals for X-ray data collection were grown from agarose gel. IR (cm^{-1}): 443m, 663s, 745m, 789s, 997w, 1134m, 1167m, 1353s, 1435m, 1506m, 1572w, 2915w. Anal. Calcd for C$_{22}$H$_{18}$CuN$_2$O$_2$ (405.93): C, 65.09; H, 4.47; N, 6.90. Found: C, 64.83; H, 4.64; N, 6.71%.

Synthesis of [Cu(5,7-Cl-8-HQ)$_2$]. A pale green solution of CuCl$_2$·2H$_2$O (100 mg, 0.58 mmol) dissolved in methanol (5 mL) was added to a solution of 5,7-dichloro-8-hydroxyquinoline (250 mg, 1.16 mmol) in 10 mL of acetone, and a dark green solid precipitated immediately. After 30 min of stirring, the solid was filtered and vacuum-dried (132 mg, yield 46%). IR (cm^{-1}): 482m, 657m, 750s, 980m, 1112m, 1254w, 1369s, 1435s, 1479m, 1539m, 1764w, 2622w, 2811w, 3049w, 3077w. Anal. Calcd for C$_{18}$H$_8$CuCl$_4$N$_2$O$_2$ (489.63): C, 44.15; H, 1.65; N, 5.72. Found: C, 44.34; H, 1.82; N, 5.56%.

Synthesis of [Cu(CQ)$_2$]. A pale green solution of CuCl$_2$·2H$_2$O (70 mg, 0.41 mmol) dissolved in methanol (5 mL) was added to a solution of clioquinol (250 mg, 0.82 mmol) in 10 mL of acetone, and a dark green solid precipitated immediately. After 30 min of stirring, the solid was filtered and vacuum-dried (207 mg, yield 75%). IR (cm^{-1}): 487m, 586m, 657s, 750s, 975m, 1112m, 1375s, 1435s, 1539m, 1753w, 2626w, 2813w, 3043w, 3069w. Anal. Calcd for C$_{18}$H$_{10}$CuCl$_2$I$_2$N$_2$O$_2$ (672.53): C, 32.15; H, 1.20; N, 4.17. Found: C, 32.33; H, 1.13; N, 4.39%.

Synthesis of [Cu(5,7-I-8-HQ)$_2$]. A pale green solution of CuCl$_2$·2H$_2$O (53 mg, 0.31 mmol) dissolved in methanol (5 mL) was added to a solution of 5,7-diiodo-8-hydroxyquinoline (250 mg, 0.62 mmol) in 20 mL of acetone/chloroform (1/1), and a green solid precipitated immediately. After 30 min of stirring, the solid was filtered and vacuum-dried (238 mg, yield 90%). IR (cm^{-1}): 482w, 657m, 750s, 980m, 1112m, 1249w, 1364s, 1435s, 1545s, 1753w, 2626w, 2813w, 3069w, 3073w. Anal. Calcd for C$_{18}$H$_8$CuI$_4$N$_2$O$_2$ (855.43): C, 25.27; H, 0.94; N, 3.27. Found: C, 25.09; H, 1.08; N, 3.17

Cell Cultures and Experimental Treatments. The HeLa cell line, derived from human cervical carcinoma, was obtained from ATCC, while human prostatic carcinoma PC3 cells were kindly provided by Prof. S. Bettuzzi (Department of Experimental Medicine, University of Parma, Italy). Cells were routinely grown in high glucose Dulbecco's modified Eagle's medium (DMEM) (4.5 g/L glucose) supplemented with 10% fetal bovine serum (FBS), 4 mM glutamine, 100 U/mL penicillin, and 100 μg/mL streptomycin.

Human umbilical vein endothelial cells (HUVECs), obtained as previously described,[71] were cultured in medium M199 supplemented with 20% fetal bovine serum (FBS), endothelial cell growth supplement (ECGS, 37.5 μg/mL), heparin (75 U/mL), and glutamine (2 mM).

Human foreskin fibroblasts (HFs) were obtained as previously described[72] and routinely grown in low glucose Dulbecco's modified Eagle's medium (DMEM) (1 g/L glucose) supplemented with 10% fetal bovine serum (FBS), 4 mM glutamine, 100 U/mL penicillin, and 100 μg/mL streptomycin.

All cells were maintained at 37 °C in a humidified atmosphere of 5% CO$_2$ in air, pH 7.4.

Ligands or copper complexes (obtained by mixing ligands and CuCl$_2$, 1:1 vol/vol, in the culture medium) were added to complete growth medium from 35 mM stock solutions in DMSO to obtain the concentrations required. Ammonium tetrathiomolybdate (TM, 10 mM in H$_2$O) was diluted to the final concentrations of 20 or 40 μM in complete growth medium. The caspase inhibitor z-VAD-FMK (10 mM in DMSO) was added to complete growth medium and used at 50 μM.

Cell Count and Viability Assay. Cells were seeded in complete growth medium in 96-well plates (7.5×10^3 cells/well) or in 24-well cell culture plates (5×10^4 cells/well) for viability assay or cell count, respectively. After 24 h, the growth medium was renewed and supplemented with the compounds as indicated by the experimental design. After 48 h of incubation under the selected conditions, cells were counted with a cell counter ZM (Coulter Electronics Ltd., Luton, U.K.) after culture trypsinization while cell viability was tested by replacing the culture medium with a solution of resazurin (110 μg/mL resazurin in PBS) in serum-free medium (1:10). Fluorescence at 572 nm was measured in each well with a fluorometer (Wallac 1420 Victor2 multilabel counter, Perkin-Elmer), and cell viability was calculated with the equation viability $= [(V_t - B)/(V_u - B)] \times 100$, where V_t and V_u are the fluorescence values obtained in treated and untreated cells, respectively, and B is the background value. Dose–response curves were fitted with nonlinear regression analysis, and IC_{50} values were calculated with GraphPad Prism 5.0.

Calculation of log P Values. The log P values of the ligands, calculated with the software ALOPGPS (VCCLAB virtual computational chemistry laboratory[73]), are in good agreement with the retention time exhibited in the reverse phase RPLC column. 5-SO₃-8-HQ was the first to elute (0.58 min) because of its marked hydrophilic character, whereas the most lipophilic ligand 5,7-I-8-HQ had the longest retention time (5.61 min) (Figure S6).

Copper Uptake. For intracellular copper determination, 1×10^6 HeLa or 1.5×10^6 PC3 cells were seeded in 100 mm dishes. After 24 h, growth medium was renewed, and the monolayers were treated as indicated in Figure 5. After the incubation, three culture plates/condition were used for analytical copper determination. Cells were rapidly washed twice with ice-cold PBS and collected in 1.5 mL of trypsin solution. The samples were diluted to 5 mL with concentrated HNO_3, mineralized by a microwave procedure, and analyzed for copper content using ICP-AES (inductively coupled plasma atomic emission spectroscopy). One culture plate/condition was used for protein quantification according to a modified Lowry method.[72] The copper content under each condition is expressed as nmol/mg protein.

Western Blot Analysis. Cells, grown to subconfluence on 10 cm diameter dishes, were treated as required by the experimental plan. At the end of the treatment, both adherent and floating cells were collected, rinsed twice in PBS, and lysed in lysis buffer containing 20 mM Tris-HCl, pH 7.5, 150 mM NaCl, 1 mM EDTA, 1 mM EGTA, 1% Triton, 2.5 mM sodium pyrophosphate, 1 mM β-glycerophosphate, 1 mM Na_3VO_4, 1 mM NaF, 2 mM imidazole, and a cocktail of protease inhibitors (cOmplete, Mini, EDTA-free, Roche). Lysates were then sonicated for 5 s and centrifuged at 12000g for 10 min at 4 °C. After protein quantification of the supernatant with the Bio-Rad protein assay, 30 μg of protein was mixed with Laemmli buffer 4×, warmed at 95 °C for 5 min, and loaded on a gel for SDS–PAGE. Resolved proteins were then transferred to polyvinylidene difluoride membranes (Millipore, Immobilon-P). After a 2 h incubation at room temperature in 10% blocking solution (Roche Diagnostics SpA, Milan, Italy), blots were exposed overnight at 4 °C to anti-caspase-3 (full-length and cleaved, rabbit polyclonal 1:1000, Cell Signaling) or anti-PARP1 (full-length and cleaved, mouse monoclonal 1:500, Santa Cruz Biotechnology) primary antibodies and diluted in a 5% bovine serum albumin solution in TBS Tween 0.1%. The blots were then washed and exposed for 1 h at room temperature to HRP-conjugated anti-mouse or anti-rabbit antibodies (ExactaCrutz, Santa Cruz Biotechnology), diluted 1:10000 in blocking solution. Immunoreactivity was visualized with the Immobilon Western chemiluminescent HRP substrate (Millipore).

Caspase-3 Activity. Cells were grown to subconfluence on 10 cm diameter dishes and treated as required. At the end of the treatment, both adherent and floating cells were collected and rinsed once in PBS. Pellets were resuspended in 500 μL of 50 mM Hepes, 0.1% CHAPS, 10 mM EDTA, 5% glycerol, and 10 mM DTT and vigorously vortexed. After centrifugation at 12000g for 10 min at 4 °C, the protein content in the supernatant was determined with the Bio-Rad protein assay and adjusted to the same concentration. Aliquots of 80 μg of protein were distributed in each well of a 96-well plate, along with the

caspase-3 substrate Ac-DEVD-pNA (200 μM, Alexis Biochemicals). The absorbance at 405 nM was read with a microplate reader (Wallac 1420 Victor2 multilabel counter, Perkin-Elmer) after 2 h at 37 °C. Caspase-3 activity under each condition is expressed as the percent of the value obtained for the untreated control cells after subtraction of the blank value.

LDH Release. Cells were grown to subconfluence on 24-well plates and treated as required. Lactate dehydrogenase (LDH), released from necrotic cells into the medium, was assessed with a CytoTox 96 nonradioactive cytotoxicity assay (Promega, Milano, Italy). The amount of LDH released was expressed as percent of LDH released from untreated cells (percent of control).

Immunofluorescence. HeLa cells (8×10^4 cells) were seeded on chamber slides and grown to subconfluence, then treated as indicated in Figures 7 and S10. Cells were then fixed in 3.7% paraformaldehyde and permeabilized with ice-cold methanol for calnexin staining or fixed and permeabilized in methanol for AIF detection. After blocking with 5% anti-goat serum, fixed cells were incubated at 4 °C overnight with rabbit polyclonal antibodies (1:50 anti-calnexin, Cell Signaling, and 1:100 anti-AIF, Santa Cruz Biotechnology). After being washed, cells were incubated with 488 Alexa Fluor goat anti-rabbit IgG antibody (1:800) and then visualized by means of a Nikon Eclipse 300 inverted fluorescence microscope (for calnexin) or a LSM 510 META Zeiss confocal microscope (for AIF).

Materials. Serum was obtained from Lonza, Basel, Switzerland. DMEM and M199 were provided by Euroclone, Italy. Z-VAD-FMK was provided by Enzo Life Sciences. Staurosporine was purchased from Sigma-Aldrich. Unless otherwise indicated, Sigma Aldrich was the source of all other chemicals, including ligands.

■ ASSOCIATED CONTENT

Ⓢ Supporting Information

Stability constants determination, competition studies with human serum albumin, X-ray structure of $[Cu(5,7\text{-Me-8-HQ})_2]$ (CCDC 891695) and crystallographic data in CIF format, cell viability assays (HeLa, PC3, HUVEC, and HF), confocal microscope images of AIF translocation. This material is available free of charge via the Internet at http://pubs.acs.org.

■ AUTHOR INFORMATION

Corresponding Author

*Phone: 0039 0521 905419. E-mail: marchio@unipr.it.

Present Address

‖The Beatson Institute for Cancer Research, Switchback Road, Glasgow G61 1BD, U.K.

Author Contributions

§These authors contributed equally.

Notes

The authors declare no competing financial interest.

■ ABBREVIATIONS USED

AIF, apoptosis inducing factor; ATP7A, copper transporting ATPase A; ATP7B, copper transporting ATPase B; CHOP, CCAAT-enhancer-binding protein homologous protein; CQ,

clioquinol; DMSO, dimethyl sulfoxide; ENDOG, endonuclease G; ER, endoplasmic reticulum; GSH, glutathione; GSSG, oxidized glutathione; hCTR1, human copper transporter 1; 8-HQ, 8-hydroxyquinoline; HSA, human serum albumin; ICP-AES, inductively coupled plasma atomic emission spectroscopy; LDH, lactate dehydrogenase; PARP-1, poly ADP-ribose polymerase-1; PCD, programmed cell death; ROS, reactive oxygen species; TM, ammonium tetrathiomolybdate; UPR, unfolded protein response; z-VAD-FMK, carbobenzoxyvalylalanylaspartyl[O-methyl]fluoromethyl ketone

■ REFERENCES

(1) Galluzzi, L.; Vitale, I.; Abrams, J. M.; Alnemri, E. S.; Baehrecke, E. H.; Blagosklonny, M. V.; Dawson, T. M.; Dawson, V. L.; El-Deiry, W. S.; Fulda, S.; Gottlieb, E.; Green, D. R.; Hengartner, M. O.; Kepp, O.; Knight, R. A.; Kumar, S.; Lipton, S. A.; Lu, X.; Madeo, F.; Malorni, W.; Mehlen, P.; Nunez, G.; Peter, M. E.; Piacentini, M.; Rubinsztein, D. C.; Shi, Y.; Simon, H. U.; Vandenabeele, P.; White, E.; Yuan, J.; Zhivotovsky, B.; Melino, G.; Kroemer, G. Molecular definitions of cell death subroutines: recommendations of the Nomenclature Committee on Cell Death. *Cell Death Differ.* **2012**, *19*, 107−120.

(2) *Apoptosis in Carcinogenesis and Chemotherapy*; Chen, G. G., Lai, P. B. S., Eds.; Springer: Dordrecht, The Netherlands, 2009.

(3) Pop, C.; Salvesen, G. S. Human caspases: activation, specificity, and regulation. *J. Biol. Chem.* **2009**, *284*, 21777−21781.

(4) Salvesen, G. S.; Ashkenazi, A. Snapshot: caspases. *Cell* **2011**, *147*, 476−476e1.

(5) Cande, C.; Vahsen, N.; Garrido, C.; Kroemer, G. Apoptosis-inducing factor (AIF): caspase-independent after all. *Cell Death Differ.* **2004**, *11*, 591−595.

(6) Susin, S. A.; Lorenzo, H. K.; Zamzami, N.; Marzo, I.; Snow, B. E.; Brothers, G. M.; Mangion, J.; Jacotot, E.; Costantini, P.; Loeffler, M.; Larochette, N.; Goodlett, D. R.; Aebersold, R.; Siderovski, D. P.; Penninger, J. M.; Kroemer, G. Molecular characterization of mitochondrial apoptosis-inducing factor. *Nature* **1999**, *397*, 441−446.

(7) Walter, P.; Ron, D. The unfolded protein response: from stress pathway to homeostatic regulation. *Science* **2011**, *334*, 1081−1086.

(8) Hetz, C. The unfolded protein response: controlling cell fate decisions under ER stress and beyond. *Nat. Rev. Mol. Cell Biol.* **2012**, *13*, 89−102.

(9) Tardito, S.; Bassanetti, I.; Bignardi, C.; Elviri, L.; Tegoni, M.; Mucchino, C.; Bussolati, O.; Franchi-Gazzola, R.; Marchiò, L. Copper binding agents acting as copper Ionophores lead to caspase inhibition and paraptotic cell death in human cancer cells. *J. Am. Chem. Soc.* **2011**, *133*, 6235−6242.

(10) Tardito, S.; Bussolati, O.; Maffini, M.; Tegoni, M.; Giannetto, M.; Dall'Asta, V.; Franchi-Gazzola, R.; Lanfranchi, M.; Pellinghelli, M. A.; Mucchino, C.; Mori, G.; Marchiò, L. Thioamido coordination in a thioxo-1,2,4-triazole copper(II) complex enhances nonapoptotic programmed cell death associated with copper accumulation and oxidative stress in human cancer cells. *J. Med. Chem.* **2007**, *50*, 1916−1924.

(11) Wasik, A. M.; Almestrand, S.; Wang, X.; Hultenby, K.; Dackland, A. L.; Andersson, P.; Kimby, E.; Christensson, B.; Sander, B. WIN55,212-2 induces cytoplasmic vacuolation in apoptosis-resistant MCL cells. *Cell Death Dis.* **2011**, *2*, e225.

(12) Yoon, M. J.; Kim, E. H.; Lim, J. H.; Kwo, T. K.; Choi, K. S. Superoxide anion and proteasomal dysfunction contribute to curcumin-induced paraptosis of malignant breast cancer cells. *Free Radical Biol. Med.* **2010**, *48*, 713−726.

(13) Yoon, M. J.; Kim, E. H.; Kwon, T. K.; Park, S. A.; Choi, K. S. Simultaneous mitochondrial Ca^{2+} overload and proteasomal inhibition are responsible for the induction of paraptosis in malignant breast cancer cells. *Cancer Lett.* **2012**, *324*, 197−209.

(14) De Feo, C. J.; Aller, S. G.; Siluvai, G. S.; Blackburn, N. J.; Unger, V. M. Three-dimensional structure of the human copper transporter hCTR1. *Proc. Natl. Acad. Sci. U.S.A.* **2009**, *106*, 4237−4242.

(15) Haas, K. L.; Putterman, A. B.; White, D. R.; Thiele, D. J.; Franz, K. J. Model peptides provide new insights into the role of histidine residues as potential ligands in human cellular copper acquisition via Ctr1. *J. Am. Chem. Soc.* **2011**, *133*, 4427−4437.

(16) Festa, R. A.; Thiele, D. J. Copper: an essential metal in biology. *Curr. Biol.* **2011**, *21*, R877−R883.

(17) Kim, B. E.; Nevitt, T.; Thiele, D. J. Mechanisms for copper acquisition, distribution and regulation. *Nat. Chem. Biol.* **2008**, *4*, 176−185.

(18) Rosenzweig, A. C.; O'Halloran, T. V. Structure and chemistry of the copper chaperone proteins. *Curr. Opin. Chem. Biol.* **2000**, *4*, 140−147.

(19) Marzano, C.; Pellei, M.; Tisato, F.; Santini, C. Copper complexes as anticancer agents. *Anti-Cancer Agents Med. Chem.* **2009**, *9*, 185−211.

(20) Tardito, S.; Marchiò, L. Copper compounds in anticancer strategies. *Curr. Med. Chem.* **2009**, *16*, 1325−1348.

(21) Price, K. A.; Crouch, P. J.; Volitakis, I.; Paterson, B. M.; Lim, S.; Donnelly, P. S.; White, A. R. Mechanisms controlling the cellular accumulation of copper bis(thiosemicarbazonato) complexes. *Inorg. Chem.* **2011**, *50*, 9594−9605.

(22) Meade, T. W. Subacute myelo-optic neuropathy and clioquinol. An epidemiological case-history for diagnosis. *Br. J. Prev. Soc. Med.* **1975**, *29*, 157−169.

(23) Cherny, R. A.; Atwood, C. S.; Xilinas, M. E.; Gray, D. N.; Jones, W. D.; Mclean, C. A.; Barnham, K. J.; Volitakis, I.; Fraser, F. W.; Kim, Y. S.; Huang, X. D.; Goldstein, L. E.; Moir, R. D.; Lim, J. T.; Beyreuther, K.; Zheng, H.; Tanzi, R. E.; Masters, C. L.; Bush, A. I. Treatment with a copper−zinc chelator markedly and rapidly inhibits beta-amyloid accumulation in Alzheimer's disease transgenic mice. *Neuron* **2001**, *30*, 665−676.

(24) Treiber, C.; Simons, A.; Strauss, M.; Hafner, M.; Cappai, R.; Bayer, T. A.; Multhaup, G. Clioquinol mediates copper uptake and counteracts copper efflux activities of the amyloid precursor protein of Alzheimer's disease. *J. Biol. Chem.* **2004**, *279*, 51958−51964.

(25) Ritchie, C. W.; Bush, A. I.; Mackinnon, A.; Macfarlane, S.; Mastwyk, M.; MacGregor, L.; Kiers, L.; Cherny, R.; Li, Q. X.; Tammer, A.; Carrington, D.; Mavros, C.; Volitakis, I.; Xilinas, M.; Ames, D.; Davis, S.; Volitakis, I.; Xilinas, M.; Ames, D.; Davis, S.; Beyreuther, K.; Tanzi, R. E.; Masters, C. L. Metal−protein attenuation with iodochlorhydroxyquin (clioquinol) targeting A beta amyloid deposition and toxicity in Alzheimer disease: a pilot phase 2 clinical trial. *Arch. Neurol.* **2003**, *60*, 1685−1691.

(26) Adlard, P. A.; Cherny, R. A.; Finkelstein, D. I.; Gautier, E.; Robb, E.; Cortes, M.; Volitakis, I.; Liu, X.; Smith, J. P.; Perez, K.; Laughton, K.; Li, Q. X.; Charman, S. A.; Nicolazzo, J. A.; Wilkins, S.; Deleva, K.; Lynch, T.; Kok, G.; Ritchie, C. W.; Tanzi, R. E.; Cappai, R.; Masters, C. L.; Barnham, K. J.; Bush, A. I. Rapid restoration of cognition in Alzheimer's transgenic mice with 8-hydroxy quinoline analogs is associated with decreased interstitial A beta. *Neuron* **2008**, *59*, 43−55.

(27) Treatment Horizon. http://www.alz.org/research/science/alzheimers_treatment_horizon.asp.

(28) Tardito, S.; Isella, C.; Medico, E.; Marchiò, L.; Bevilacqua, E.; Hatzoglou, M.; Bussolati, O.; Franchi-Gazzola, R. The thioxotriazole copper(II) complex A0 induces endoplasmic reticulum stress and paraptotic death in human cancer cells. *J. Biol. Chem.* **2009**, *284*, 24306−24319.

(29) Ding, W. Q.; Lind, S. E. Metal ionophores: an emerging class of anticancer drugs. *IUBMB Life* **2009**, *61*, 1013−1018.

(30) Ding, W. Q.; Liu, B. L.; Vaught, J. L.; Yamauchi, H.; Lind, S. E. Anticancer activity of the antibiotic clioquinol. *Cancer Res.* **2005**, *65*, 3389−3395.

(31) Ammor, S.; Coquerel, G.; Perez, G.; Robert, F. Synthesis, thermal-behavior and crystal-structure of a tetrahydrated copper(II) 5-sulfonic-8-quinolinolato complex with a 2-dimensional polymeric structure. *Eur. J. Solid State Inorg. Chem.* **1992**, *29*, 131−139.

(32) Francis, S.; Muthiah, P. T.; Bocelli, G.; Cantoni, A. Polymeric diaqua(mu-8-hydroxy-7-iodo-quinoline-5-sulfonato-kappa *N*-

4,O,O′,O″)copper(II) tetrahydrate. *Acta Crystallogr., Sect. E: Struct. Rep. Online* **2003**, *59*, M1157−M1159.

(33) Petit, S.; Coquerel, G.; Perez, G.; Louer, D.; Louer, M. Abinitio crystal-structure determination of dihydrated copper(II) 5-sulfonic-8-quinolinolato complex (form-I) from X-Ray-powder diffraction data: filiations with related copper(II) sulfoxinates. *New J. Chem.* **1993**, *17*, 187−192.

(34) Ammor, S.; Coquerel, G.; Perez, G.; Robert, F. Structure of the gamma′ form of copper(II) quinolinolate and structural filiations to related M²⁺ complexes. *Eur. J. Solid State Inorg. Chem.* **1992**, *29*, 445−453.

(35) Di Vaira, M.; Bazzicalupi, C.; Orioli, P.; Messori, L.; Bruni, B.; Zatta, P. Clioquinol, a drug for Alzheimer's disease specifically interfering with brain metal metabolism: structural characterization of its zinc(II) and copper(II) complexes. *Inorg. Chem.* **2004**, *43*, 3795−3797.

(36) Stary, J.; Zolotov, Y. A.; Petrukhin, O. M. *Critical Evaluation of Equilibrium Constants Involving 8-Hydroxyquinoline and Its Metal Chelates*; IUPAC Chemical Data Series 24; Pergamon Press: Oxford, U.K., 1979; pp 18−55.

(37) Ahmed, I. T.; Boraei, A. A. A.; El-Roudi, O. M. Mixed-ligand complexes of some divalent transition metal ions with dicarboxylic amino acids and 8-hydroxyquinoline. *J. Chem. Eng. Data* **1998**, *43*, 459−464.

(38) Nakamura, H.; Yoshida, T.; Todoko, M.; Ueno, K.; Takagi, M. Syntheses and chelating properties of sulfonamidoquinolines. *Bull. Chem. Soc. Jpn.* **1984**, *57*, 2839−2846.

(39) Sawicka, J.; Youyou, N.; Swiatek, J.; Decock, P.; Kozlowski, H.; Blondeau, D.; Lenormand, I. Synthesis and coordination ability of substituted imidazo-pyridines, structural analogs of oxine: influence of copper(II) and nickel(II) ions on toxicity of the organic ligand. *J. Inorg. Biochem.* **1991**, *44*, 117−125.

(40) Smith, R. M.; Martell, A. E.; Motekaitis, R. J. *NIST Critically Selected Stability Constants of Metal Complexes Database*; National Institute of Standards and Technology: Gaithersburg, MD, 2007.

(41) Pettit, L. D.; Powell, H. K. J. *The IUPAC Stability Constants Database*; IUPAC: Research Triangle Park, NC, 2000.

(42) Aquilanti, G.; Giorgetti, M.; Minicucci, M.; Papini, G.; Pellei, M.; Tegoni, M.; Trasatti, A.; Santini, C. A study on the coordinative versatility of new N,S-donor macrocyclic ligands: XAFS, and Cu²⁺ complexation thermodynamics in solution. *Dalton Trans.* **2011**, *40*, 2764−2777.

(43) National Institutes of Health. http://www.nih.gov/.

(44) Ruschak, A. M.; Slassi, M.; Kay, L. E.; Schimmer, A. D. Novel proteasome inhibitors to overcome bortezomib resistance. *J. Natl. Cancer Inst.* **2011**, *103*, 1007−1017.

(45) Schimmer, A. D. Clioquinol: a novel copper-dependent and independent proteasome inhibitor. *Curr. Cancer Drug Targets* **2011**, *11*, 325−331.

(46) Cater, M. A.; Haupt, Y. Clioquinol induces cytoplasmic clearance of the X-linked inhibitor of apoptosis protein (XIAP): therapeutic indication for prostate cancer. *Biochem. J.* **2011**, *436*, 481−491.

(47) Brewer, G. J.; Dick, R. D.; Yuzbasiyangurkin, V.; Tankanow, R.; Young, A. B.; Kluin, K. J. Initial therapy of patients with Wilsons-disease with tetrathiomolybdate. *Arch. Neurol.* **1991**, *48*, 42−47.

(48) Ding, X.; Xie, H.; Kang, Y. J. The significance of copper chelators in clinical and experimental application. *J. Nutr. Biochem.* **2011**, *22*, 301−310.

(49) Kaufmann, S. H.; Desnoyers, S.; Ottaviano, Y.; Davidson, N. E.; Poirier, G. G. Specific proteolytic cleavage of poly(ADP-ribose) polymerase: an early marker of chemotherapy-induced apoptosis. *Cancer Res.* **1993**, *53*, 3976−3985.

(50) Lazebnik, Y. A.; Kaufmann, S. H.; Desnoyers, S.; Poirier, G. G.; Earnshaw, W. C. Cleavage of poly(ADP-ribose) polymerase by a proteinase with properties like ice. *Nature* **1994**, *371*, 346−347.

(51) Nicolier, M.; Decrion-Barthod, A. Z.; Launay, S.; Prétet, J. L.; Mougin, C. Spatiotemporal activation of caspase-dependent and -independent pathways in staurosporine-induced apoptosis of p53wt and p53mt human cervical carcinoma cells. *Biol. Cell* **2009**, *101*, 455−467.

(52) Chen, D.; Cui, Q. C.; Yang, H. J.; Barrea, R. A.; Sarkar, F. H.; Sheng, S. J.; Yan, B.; Reddy, G. P. V.; Dou, Q. P. Clioquinol, a therapeutic agent for Alzheimer's disease, has proteasome-inhibitory, androgen receptor-suppressing, apoptosis-inducing, and antitumor activities in human prostate cancer cells and xenografts. *Cancer Res.* **2007**, *67*, 1636−1644.

(53) Banci, L.; Bertini, I.; Ciofi-Baffoni, S.; Kozyreva, T.; Zovo, K.; Palumaa, P. Affinity gradients drive copper to cellular destinations. *Nature* **2010**, *465*, 645−648.

(54) Xiao, Z. G.; Brose, J.; Schimo, S.; Ackland, S. M.; La Fontaine, S.; Wedd, A. G. Unification of the copper(I) binding affinities of the metallo-chaperones Atx1, Atox1, and related proteins: detection probes and affinity standards. *J. Biol. Chem.* **2011**, *286*, 11047−11055.

(55) Ishida, S.; Lee, J.; Thiele, D. J.; Herskowitz, I. Uptake of the anticancer drug cisplatin mediated by the copper transporter Ctr1 in yeast and mammals. *Proc. Natl. Acad. Sci. U.S.A.* **2002**, *99*, 14298−14302.

(56) Wang, D.; Lippard, S. J. Cellular processing of platinum anticancer drugs. *Nat. Rev. Drug Discovery* **2005**, *4*, 307−320.

(57) Veldman, R. J.; Zerp, S.; van Blitterswijk, W. J.; Verheij, M. *N*-Hexanoyl-sphingomyelin potentiates in vitro doxorubicin cytotoxicity by enhancing its cellular influx. *Br. J. Cancer* **2004**, *90*, 917−925.

(58) Wilson, J. J.; Lippard, S. J. In vitro anticancer activity of cis-diammineplatinum(II) complexes with β-diketonate leaving group ligands. *J. Med. Chem.* **2012**, *55*, 5326−5336.

(59) Giannini, F.; Furrer, J.; Ibao, A.-F.; Suss-Fink, G.; Therrien, B.; Zava, O.; Baquie, M.; Dyson, P. J.; Stepnicka, P. *J. Biol. Inorg. Chem.* **2012**, *17*, 951−960.

(60) Rohde, W.; Mikelens, P.; Jackson, J.; Blackman, J.; Whitcher, J.; Levinson, W. Hydroxyquinolines inhibit ribonucleic acid-dependent deoxyribonucleic acid polymerase and inactivate Rous sarcoma virus and herpes simplex virus. *Antimicrob. Agents Chemother.* **1976**, *10*, 234−240.

(61) Gouras, G. K.; Beal, M. F. Metal chelator decreases Alzheimer beta-amyloid plaques. *Neuron* **2001**, *30*, 641−642.

(62) Zhai, S. M.; Yang, L.; Cui, Q. C.; Sun, Y.; Dou, Q. P.; Yan, B. Tumor cellular proteasome inhibition and growth suppression by 8-hydroxyquinoline and clioquinol requires their capabilities to bind copper and transport copper into cells. *J. Biol. Inorg. Chem.* **2010**, *15*, 259−269.

(63) Kumar, P.; Yadav, A.; Patel, S. N.; Islam, M.; Pan, Q. T.; Merajver, S. D.; Teknos, T. N. Tetrathiomolybdate inhibits head and neck cancer metastasis by decreasing tumor cell motility, invasiveness and by promoting tumor cell anoikis. *Mol. Cancer* **2010**, *9*, 206.

(64) Juarez, J. C.; Betancourt, O.; Pirie-Shepherd, S. R.; Guan, X. J.; Price, M. L.; Shaw, D. E.; Mazar, A. P.; Donate, F. Copper binding by tetrathiomolybdate attenuates angiogenesis and tumor cell proliferation through the inhibition of superoxide dismutase 1. *Clin. Cancer Res.* **2006**, *12*, 4974−4982.

(65) Jiang, H. C.; Taggart, J. E.; Zhang, X. X.; Benbrook, D. M.; Lind, S. E.; Ding, W. Q. Nitroxoline (8-hydroxy-5-nitroquinoline) is more a potent anti-cancer agent than clioquinol (5-chloro-7-iodo-8-quinoline). *Cancer Lett.* **2011**, *312*, 11−17.

(66) Daniel, K. G.; Chen, D.; Orlu, S.; Cui, Q. C.; Miller, F. R.; Dou, Q. P. Clioquinol and pyrrolidine dithiocarbamate complex with copper to form proteasome inhibitors and apoptosis inducers in human breast cancer cells. *Breast Cancer Res.* **2005**, *7*, R897−R908.

(67) Moubarak, R. S.; Yuste, V. J.; Artus, C.; Bouharrour, A.; Greer, P. A.; Murcia, J. M. D.; Susin, S. A. Sequential activation of poly(ADP-ribose) polymerase 1, calpains, and bax is essential in apoptosis-inducing factor-mediated programmed necrosis. *Mol. Cell. Biol.* **2007**, *27*, 4844−4862.

(68) Vandenabeele, P.; Galluzzi, L.; Vanden Berghe, T.; Kroemer, G. Molecular mechanisms of necroptosis: an ordered cellular explosion. *Nat. Rev. Mol. Cell Biol.* **2010**, *11*, 700−714.

(69) Tardito, S.; Bussolati, O.; Gaccioli, F.; Gatti, R.; Guizzardi, S.; Uggeri, J.; Marchiò, L.; Lanfranchi, M.; Franchi-Gazzola, R. Non-

apoptotic programmed cell death induced by a copper(II) complex in human fibrosarcoma cells. *Histochem. Cell Biol.* **2006**, *126*, 473−482.

(70) Gandin, V.; Pellei, M.; Tisato, F.; Porchia, M.; Santini, C.; Marzano, C. A novel copper complex induces paraptosis in colon cancer cells via the activation of ER stress signalling. *J. Cell. Mol. Med.* **2012**, *16*, 142−151.

(71) Sala, R.; Rotoli, B. M.; Colla, E.; Visigalli, R.; Parolari, A.; Bussolati, O.; Gazzola, G. C.; Dall'Asta, V. Two-way arginine transport in human endothelial cells: TNF-alpha stimulation is restricted to system y(+). *Am. J. Physiol.: Cell Physiol.* **2002**, *282*, C134−C143.

(72) Gazzola, G. C.; Dall'Asta, V.; Franchi-Gazzola, R.; White, M. F. The cluster-tray method for rapid measurement of solute fluxes in adherent cultured cells. *Anal. Biochem.* **1981**, *115*, 368−374.

(73) Virtual Computational Chemistry Laboratory. http://www.vcclab.org/.